Elucidation of the Chemical Role of the Pyroclastic Materials on the State of Conservation of Mural Paintings from Pompeii, Italy

Silvia Pérez-Diez,*[a] Luis Javier Fernández-Menéndez,[b] Héctor Morillas,[a][c] Alberta Martellone,[d] Bruno De Nigris,[d] Massimo Osanna,[e] Nerea Bordel,[b] Juan Manuel Madariaga[a] and Maite Maguregui*[f]

Abstract: Pyroclastic strata have always been thought to protect the archaeological remains of the Vesuvian area (Italy), hence allowing their conservation throughout the centuries. In this work, we demonstrate that they constitute a potential threat for the conservation state of the mural paintings of Pompeii. The ions that could be leached from them, together with the influence of the groundwater rich in ions coming from the volcanic soil/rocks, may contribute to the crystallisation of salts. Thermodynamic modelling not only allowed to predict which salts can precipitate from these leaching events, but also assisted the identification of additional sources of mainly sulfates and alkali metals, to explain the formation of the sulfates identified in efflorescences from the mural paintings of Pompeii. For the future, fluorine, only related to a volcanic origin, can be proposed as a marker to monitor in situ the extension of the impact in the mural paintings of Pompeii.

Table of Contents

Experimental Procedures

Samples

Table S2. Pyroclastic materials sampled at the Archaeological Park of Pompeii.

Stratigraphy	Stratum	Type of sample
Necropoli di Porta Nola (VN)	2	Ash and lapilli
	3	Ash and lapilli
	4	Ash and lapilli
	5	Lapilli
Porta di Stabia (PS)	1	Ash
	2	Lapilli
	3	Lapilli
	4	Ash and lapilli
	5	Ash
	6	Ash and lapilli
	7	Ash
	8	Lapilli
Insula dei Casti Amanti (CA)	1	Lapilli
	2	Lapilli
	3	Lapilli
	4	Lapilli
	5	Ash
	7	Lapilli
Porta Marina	1	Completely ground
	2	Completely ground
	3	Completely ground
	4	Completely ground
	5	Completely ground
	7	Completely ground
ASH	-	Ash (and lapilli)
LAP	-	Lapilli
ARI	-	Lapilli

According to visual observations and archaeologists' opinion, the ASH sample was presumably mixed with soil and lapilli.

Additionally, an efflorescence sampled at the triclinium of the House of Marcus Lucretius (S1; Regio IX, 3, 5) and an efflorescence sampled at the exedra (Room 22) of the House of Ariadne (S2; Regio VII, 4, 31/51) were considered for this study.

Sample preparation

For the LIBS measurements pyroclastic materials were manually ground in an agate mortar and pressed pellets of the ground material were prepared using a manual hydraulic press at 20 tons.

The leaching procedure of the pyroclastic materials was designed according to the recommendations of the International Volcanic Health Hazard Network (IVHHN).[1] Deionised water was employed as leaching agent to dissolve the water-soluble compounds adsorbed onto the surface of the materials. Non-ground samples and a 1:20 ratio were preferred in order to recreate the real situation in the archaeological site (direct leaching of the pyroclastic materials as they were deposited in the burial).
The protocol is as follows: 1 g of volcanic material was stirred (700 rpm) during one hour in deionised water (1:20) and subsequently filtered and stored in the refrigerator prior to the Ion Chromatography analyses. Each sample was leached in triplicate.

The efflorescence samples were analysed directly by means of the LIBS and Raman micro-spectroscopy and they were ground for the XRD measurements.

Pressed pellets of pure reference compounds (CaO, $CaCl_2$ and CaF_2) were prepared using a manual hydraulic press at 20 tons.

Materials

Calcium carbonate (99.999 % trace metals basis), calcium chloride dehydrate (Reagent Plus® > 99.0 %) were purchased from Sigma Aldrich, whereas calcium fluoride (> 99.5 %) was purchased from Alfa Aesar.

Instrumentation

X-Ray Diffraction (XRD)

The analyses were performed with a PANalytical X'pert PRO powder diffractometer equipped with a copper tube ($\lambda Cu_{K\alpha mean}$ = 1.5418 Å, $\lambda Cu_{K\alpha 1}$ = 1.54060 Å, $\lambda Cu_{K\alpha 2}$ = 1.54439 Å), vertical goniometer (Bragg–Brentano geometry), programmable divergence aperture, automatic sample changer, secondary graphite monochromator and PixCel detector. The operating conditions for the Cu tube were 40 kV and 40 mA, and the angular range (2θ) was scanned between 5° and 70°. The treatment of the diffractogram data were carried out using X'pert HighScore Plus software.
All the previously described samples were manually ground in an agate mortar to perform the analyses.

Raman spectroscopy

The inVia confocal Raman microscope (Renishaw, Gloucestershire, UK) was used for single point molecular analysis. This instrument is equipped with a Peltier-cooled CCD detector (-70 °C). The spectrometer is coupled to DMLM Leica microscope, which can use a great variety of long-range lens (5x, 20x, 50x and 100x). The confocality allows to obtain the maximum lateral resolution of the microscope. The microscope is equipped with a motorized XYZ positioning stage with integrated position sensors on the X and Y axes (Renishaw). Excitation lasers of 785 and 532 nm were used for measuring. The spectra were acquired in the 60-1200 cm^{-1} or 200-2200 cm^{-1} spectral range and accumulated 3, 5 or 10 times.

Laser Induced Breakdown Spectroscopy (p-LIBS)

The portable LIBS (p-LIBS) employed for this study was the EasyLIBS IVEA (model Easy 2C) LIBS system. This instrument employs a pulsed Nd:YAG laser, with the possibility of operating in a dual pulse mode, emitting at a wavelength of 1064 nm. The laser energy per pulse on the sample is lower than 25 mJ with a repetition rate of 1 Hz. The Easy 2C model consists of an optic probe that allows focusing the laser connected to a computer and to three spectrometers covering the ultraviolet (UV, 196–419 nm), the visible (VIS, 420–579 nm) and near infrared (NIR, 580–1000 nm) spectral ranges respectively. The software used for automatic acquisition, control, visualisation and processing of the spectra was the AnaLIBS version 6.3. The analyses were performed directly placing the sampling interface on the surface under study. Data interpretation was carried out using the NIST database.

The acquisition parameters for the detection of CaF and CaCl molecular bands in the portable commercial LIBS were the following: gate width of 100 ms and a delay time of 3 µs. At least 20 spectra were acquired in each pellet to ensure a representative result.

Laser Induced Breakdown Spectroscopy (benchtop LIBS)

A non-commercial benchtop LIBS system which implements a Nd:YAG laser (EKSPLA, NL301HT) operating at 1064 nm, with pulse duration of 4.5 ns, was used to obtain the spectra of the pyroclastic materials in the laboratory. The laser pulse energy was set to 100 mJ/pulse using an attenuator (LOTIS-TII), and the laser repetition rate was fixed at 10 Hz. The laser beam was focused in the sample surface using an objective with 35 mm of focal length (Thorlabs; LMH-5X-1064). It is possible to move the sample, since it is placed on a X-Y stage controlled by two stepper motors (PImiCos GmbH VT_80200-2SM and another one manufactured by the University of Oviedo) working at a velocity of 4 mm/s, while the lens-to-sample distance was kept by using a laser distance measurer (MicroEpsilon optoNCTD 1402) with a maximum resolution of 0.6 µm.
Plasma emission was collected by two plano-convex lenses (Thorlabs, LA4904-UV and LA4855-UV), directly forming the plasma image on the entrance of the Czerny–Turner spectrometer (Andor Shamrock SR-500i-D1). This device has 2 diffraction gratings, one of 1200 lines/mm (allowing the detection of a 30 nm broadband spectrum) and the other with 2400 lines/mm (allowing the detection of a 15 nm broadband spectrum with higher resolution). Emission signals were finally recorded using an iCCD camera (Andor iStar DH734-25F-03) with 1024 × 1024 pixels that have an effective size per pixel of 19.5 × 19.5 µm.

The acquisition parameters conditions for the detection of CaF and CaCl molecular bands in the benchtop LIBS were the following: gate width of 100 µs and a delay time of 30 µs. Two rasters of 12 laser pulses were acquired in each of the two spectral windows (one centered in 530 nm and the other one in 590 nm).

Ion chromatography (IC)

The chromatographic analyses were performed using a 930 Compact IC Flex equipment (Metrohm). The anion column is a Metrosep A Supp 7 – 150/4.0 mm, which can operate between 3 and 12 pH values and 20-60 ºC, with a standard temperature of 45 ºC and at a maximum pressure of 15 MPa (150 bar). The maximum flux is 1 mL/min (eluent: 3.6 mmol/L sodium carbonate). It is equipped with a pre-column Metrosep A Supp 5 Guard/4.0. The cation column is a Metrosep C 6– 150/4.0 mm, which can operate between 2 and 7 pH values and at a maximum pressure of 20 MPa (200 bar). The maximum flux is 0.9 mL/min (eluent: 1.7 mmol/L nitric acid + 1.7 mmol/L dipicolinic acid). It is equipped with a pre-column Metrosep C 6 Guard/4.0. The 930 Compact IC Flex chromatograph has two suppressor modules: Metrohm Suppressor Module (MSM) C and A.

pH meter

For the pH measurements, a Metrohm 692 pH/Ion Meter was used (calibrated before any measurement of the leached extracts).

Correlation analysis

To determine the relationship between the anions and cations quantified in the leachates from the pyroclastic materials, the Pearson correlation coefficients were calculated using The Unscrambler® 7.6 softwaere (CAMO software, Oslo, Norway).

Thermodynamic calculations: PHREEQC software

The PHREEQC software was employed to estimate the different salt crystallisation mechanisms, including the crystallisation pressure according to the saturation index. The calculations were based on the Wateq4f database, which was modified in order to include the following compounds: arcanite (K_2SO_4), niter (KNO_3), aphthitalite ($NaK_3(SO_4)_2$), görgeyite ($K_2Ca_5(SO4)_6.H_2O$), bischofite ($MgCl_2 \cdot 6H_2O$), polyhalite ($K_2MgCa_2(SO_4)_4 \cdot 2H_2O$) and syngenite ($K_2Ca(SO_4)_2 \cdot H_2O$), absent from the original database but already included in other databases of the software. The thermodynamic modelling was executed on the concentration values obtained via ion chromatography after the leaching procedure of the pyroclastic deposits, considered as multicomponent aqueous solutions with the following systems: Na^+–NH_4^+–K^+–Ca^{2+}–Mg^{2+}–F^-–Cl^-–Br^-–NO_2^-–NO_3^-–PO_4^{3-}–SO_4^{2-}.

The calculations were run both at 10 and 25 ºC and charge was balanced through alkalinity. In order to estimate the contribution of other inputs (e.g. groundwater, restoration mortars) to the leaching of these pyroclastic materials at the Archaeological Park of Pompeii, the Na^+, K^+, Cl^- and SO_4^{2-} concentrations were also multiplied by a factor of 25, 50, 75 and 100.

Results and Discussion

X-ray Diffraction (XRD)

Table S3. Summary of the mineralogical phases identified in each pyroclastic strata.

Stratum	Glass	Calcite (CaCO$_3$)	Quartz (α-SiO$_2$).	Pyroxenes (e.g. diopside (CaMgSi$_2$O$_6$))	Analcime (Na(AlSi$_2$O$_6$)·H$_2$O)	Leucite (KAlSi$_2$O$_6$),	Plagioclase (e.g. albite (NaAlSi$_3$O$_8$))	Sanidine (KAlSi$_3$O$_8$)	Dolomite (CaMg(CO$_3$)$_2$)	Phyllosilicates (micaceous materials)
ASH	X	X	X	X	X	X	X			X
LAP	X	X	X	X	X	X	X			X
ARI	X	X	X	X	X	X	X			X
PM 1	X	X		X	X	X	X			X
PM 2	X			X	X	X	X			X
PM 3	X			X	X	X	X			X
PM 4	X	X		X	X	X	X			X
PM 5	X	X		X	X	X	X			X
PM 7	X	X		X	X	X	X			X
PS 1		X		X	X	X	X	X	X	X
PS 2		X		X	X	X	X	X	X	X
PS 3		X		X	X	X	X	X	X	X
PS 4		X		X	X	X	X	X	X	X
PS 5		X		X	X	X	X	X		X
PS 6		X		X	X	X	X	X		X
PS 7		X		X	X	X	X	X		X
PS 8				X		X				X
VN2		X		X		X	X	X		X
VN 3		X		X		X	X	X		X

6

VN 4	X	X		X	X	X		X
VN 5		X		X				X
CA 1	X	X	X	X	X	X	X	X
CA 2	X	X	X	X	X	X	X	X
CA 3	X	X	X	X	X	X	X	X
CA 4	X	X	X	X	X	X	X	X
CA 5	X	X	X	X	X	X		X
CA 7		X	X	X				X

Apart from silicates of volcanic origin, calcite ($CaCO_3$) was also identified in almost all pyroclastic materials from all locations. Calcite may be an alteration product or the consequence of the mixing of the ashes with other materials. It has been demonstrated that calcitic nodules, which were removed from the sedimentary basement by the magma arising along the volcanic pipe,[2] have a pyroclastic origin in pozzolana aggregates of Pompeian mortars.[3]

Similarly, quartz (α-SiO_2), which was only detected in samples ASH, LAP and ARI, could have a pyroclastic origin or be an external contribution. However, the generation of quartz in feldspathoids-rich igneous rocks in the same crystallisation process is excluded because the feldspathoids are formed with low silicon concentrations, whereas quartz needs an excess of silicon to crystallise.[4] Nonetheless, quartz can be present as a secondary mineral of a previously formed volcanic rock, as a weathering product of the silicates or due to the devitrification of the volcanic glass.[5] Certain strata of Porta di Stabia (PS 1-4) and Casti Amanti (CA 1-4) also presented dolomite, $CaMg(CO_3)_2$.

Raman micro-spectroscopy

The pyroclastic strata were analysed by Raman micro-spectroscopy to detect other crystalline species in the volcanic strata, probably at lower concentrations than 1 % bearing in mind the XRD results. In this document, Raman observations have been restricted to PS 1 and VN 3 considering them as representative samples. In agreement with the XRD analysis of PS 1, both calcite and dolomite were detected (bands at 283.3 and 1088.4 cm^{-1} and 1098.0 cm^{-1}, respectively). Additionally, other fluorescence broad bands attributed to unknown silicates were identified between 1200 and 1650 cm^{-1}.

On the other hand, VN 3 presented the Raman bands of calcite (281.3, 1086.9 cm^{-1}) and the absence of dolomite, as expected according to the XRD study. Other additional phases were identified in this sample, such as leucite ($K(Si_2Al)O_6$, 493.7 and 526.5 cm^{-1}), hematite (Fe_2O_3, 219.1, 399.9 cm^{-1}), goethite (μ-FeOOH, 384.6 cm^{-1}) and magnetite (Fe_3O_4, 302.8, 668.7 cm^{-1}).[6] A band at 997.3 cm^{-1} is also present. This could be ascribed either to the (n_1) PO_4 symmetric stretching mode of certain phosphates,[7] or to the SO_4 symmetric stretching of natrochalcite, ($NaCu_2(SO_4)_2(OH, H_2O)_2$.[8]

No other Raman bands attributable to fluorine or chlorine phases were detected in all the pyroclastic strata.

Halides detection in the pyroclastic strata using portable and benchtop LIBS

Laser Induced Breakdown Spectroscopy (p-LIBS)

Concerning CaCl, there are two molecular systems in the 580-630 nm spectral range (Figure 2): the orange system (580.99 and 593.40 nm, being the latter the most intense) and the red system (605.16, 607.66, 618.49, 619.34, 621.16, 622.49, 632.58 and 635.35 nm).[9] The red system of CaCl diatomic molecules are prone to be interfered by the orange system of the molecular emission of CaO, as shown in Figure 2.[9] The orange systems of both CaCl and CaF molecular systems, when compared to the CaO emission, are adequate to identify the presence of halides in the samples. Hence, in this work, this will be the preferred spectral range for the sake of comparison.

The CaF orange system, measured with the p-LIBS, was integrated between 598.5 and 607.5 nm and the contribution of the CaO orange system was subtracted. The CaCl orange system was integrated between 592 and 594 nm. Spectra were normalised to the background and integrated using the Spectragryph software.[10]

Figure S1. LIBS spectra of the orange system of CaCl in Pompeian pyroclastic material acquired with the p-LIBS and compared with the reference spectrum of $CaCl_2$ acquired with the p-LIBS in the same conditions.

Table S3. Integrated intensities of the CaF and the CaCl orange systems in samples ASH, LAP and ARI, measured with the portable LIBS instrument.

Stratum	CaF (a.u.)	CaCl (a.u.)
ASH	9 ± 3	0.009 ± 0.006
LAP	15 ± 4	0.007 ± 0.004
ARI	4 ± 2	0.011 ± 0.008

Table S4. Integrated intensities of the CaF and the CaCl orange systems in samples CA 1-CA 7, measured with the portable LIBS instrument.

Stratum	CaF (a.u.)	CaCl (a.u.)
CA 1	5 ± 2	n.d.[a]
CA 2	11 ± 4	0.009 ± 0.005
CA 3	7 ± 2	0.006 ± 0.002
CA 4	12 ± 3	0.008 ± 0.004
CA 5	7 ± 2	0.008 ± 0.004
CA 7	12 ± 3	0.011 ± 0.009

[a] n.d., non-detected

Table S5. Integrated intensities of the CaF and the CaCl orange systems in samples PM 1-PM 7, measured with the portable LIBS instrument.

Stratum	CaF (a.u.)	CaCl (a.u.)
PM 1	8 ± 3	0.012 ± 0.007
PM 2	3 + 2	n.d.[a]
PM 3	2 ± 2	n.d.[a]
PM 4	8 ± 2	0.008 ± 0.005
PM 5	8 ± 3	0.008 ± 0.005
PM 7	9 ± 2	0.020 ± 0.009

[a] n.d., non-detected

Table S6. Integrated intensities of the CaF and the CaCl orange systems in samples PS 1-PS 8, measured with the portable LIBS instrument.

Stratum	CaF (a.u.)	CaCl (a.u.)
PS 1	10 ± 4	0.011 ± 0.006
PS 2	9 ± 3	0.011 ± 0.005
PS 3	10 ± 2	0.018 ± 0.007
PS 4	16 ± 10	0.015 ± 0.009
PS 5	11 ± 3	0.007 ± 0.004
PS 6	14 ± 4	0.011 ± 0.008
PS 7	10 ± 3	0.019 ± 0.007
PS 8	14 ± 5	0.011 ± 0.006

Table S7. Integrated intensities of the CaF and the CaCl orange systems in samples VN 2-VN 5, measured with the portable LIBS instrument.

Stratum	CaF (a.u.)	CaCl (a.u.)
VN 2	6 ± 2	0.007 ± 0.004
VN 3	16 ± 6	0.009 ± 0.006
VN 4	10 ± 3	0.011 ± 0.007
VN 5	3 ± 2	0.009 ± 0.005

Laser Induced Breakdown Spectroscopy (benchtop LIBS)

In order to evaluate the performance of the p-LIBS, the stratigraphy of Porta Marina was analysed with the benchtop LIBS. Here, the comparison between the p-LIBS and the benchtop LIBS spectrum of PM 2 is presented: the head of the CaCl orange system at 593.40 nm can be seen in the spectra of PM 2 recorded with to the benchtop instrument, but is undetected in the spectra acquired with the p-LIBS. This points out to a lower CaCl detection sensitivity in the case of the p-LIBS.

Figure S2. Comparison of the p-LIBS spectrum and the benchtop LIBS spectrum of stratum 2 of Porta Marina.

The CaF orange system was integrated between 598.5 and 607.5 nm and the baseline was subtracted. The CaCl orange system was integrated between 592 and 594 nm. Spectra were normalised to the background and integrated using the Spectragryph software.[10] The estimated RSD is about 10 %.
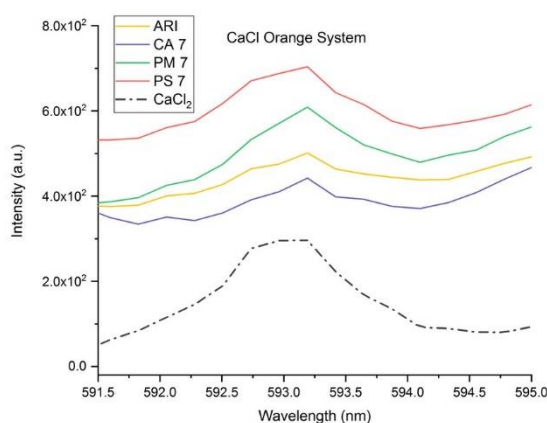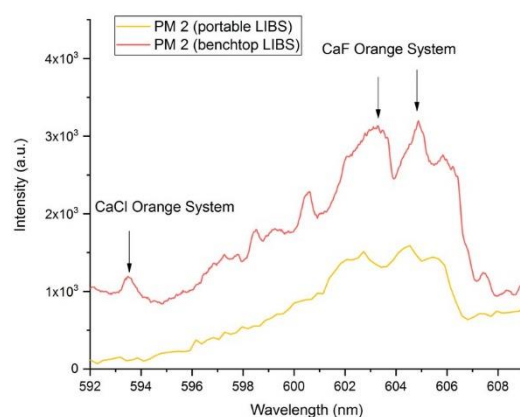
Table S4. Integrated intensities of the CaF and the CaCl orange systems in samples PM 1-PM 7, measured with the benchtop LIBS instrument.

Stratum	CaF (a.u.)	CaCl (a.u.)
PM 1	1.5	0.45
PM 2	1.1	0.15
PM 3	0.8	0.05
PM 4	2.5	0.08
PM 5	2.2	0.27
PM 7	2.0	0.94

Ion Chromatography (IC)

Table S5. ASH, LAP and ARI leachates cations concentration given in mg/L, determined via ion chromatography.

Cation	ASH	LAP	ARI
Na^+	2.72 ± 0.04	1.0 ± 0.3	10.3 ± 0.5
NH_4^+	0.006 ± 0.003	0.012 ± 0.002	0.03 ± 0.01
K^+	7.8 ± 0.3	1.3 ± 0.2	29.6 ± 0.5
Ca^{2+}	14 ± 4	12.56 ± 0.01	120 ± 10

Table S6. ASH, LAP and ARI leachates anions concentration given in mg/L, determined via ion chromatography.

Anion	ASH	LAP	ARI
F^-	0.57 ± 0.04	0.14 ± 0.04	0.79 ± 0.02
Cl^-	0.92 ± 0.06	0.5 ± 0.1	89 ± 8
NO_2^-	0.027 ± 0.04	0.014 ± 0.001	0.02 ± 0.01
Br^-	0.005 ± 0.002	0.006 ± 0.001	0.13 ± 0.02

NO$_3^-$	0.1469 ± 0.0003	0.15 ± 0.04	231 ± 16
PO$_4^{3-}$	0.051 ± 0.002	0.056 ± 0.004	0.19 ± 0.03
SO$_4^{2-}$	1.06 ± 0.07	0.20 ± 0.02	114 ± 19

Table S7. CA 1-CA 7 leachates cations concentration given in mg/L, determined via ion chromatography.

Cation	CA 1	CA 2	CA 3	CA 4	CA 5	CA 7
Na$^+$	7.89 ± 0.05	3.4 ± 0.7	9 ± 3	2.6 ± 0.1	11.0 ± 0.4	9 ± 1
NH$_4^+$	0.04 ± 0.04	0.06 ± 0.05	0.02 ± 0.01	0.010	0.02 ± 0.01	0.03 ± 0.02
K$^+$	19 ± 1	8 ± 2	24 ± 5	7.1 ± 0.6	23.5 ± 0.4	21 ± 3
Ca^{2+}	8 ± 4	17.85 ± 0.01	6 ± 8	15 ± 1	4 ± 6	20.6 ± 0.8

Table S8. CA 1-CA 7 leachates anions concentration given in mg/L, determined via ion chromatography.

Anion	CA 1	CA 2	CA 3	CA 4	CA 5	CA 7
F$^-$	1.3 ± 0.2	0.7 ± 0.2	1.0 ± 0.3	0.26 ± 0.04	0.90 ± 0.04	0.5 ± 0.1
Cl$^-$	0.86 ± 0.08	2.2 ± 0.5	4 ± 1	2.5 ± 0.3	3.68 ± 0.06	30 ± 4
NO$_2^-$	0.03 ± 0.01	0.02 ± 0.01	0.03 ± 0.01	0.02 ± 0.01	0.03	0.05 ± 0.01
Br$^-$	< LOQ[a]	0.01	0.03 ± 0.01	0.02	0.01	0.07 ± 0.01
NO$_3^-$	0.23 ± 0.04	1.9 ± 0.3	8 ± 2	2.2 ± 0.5	3.8 ± 0.2	27 ± 4
PO$_4^{3-}$	0.03 ± 0.01	0.02	0.05 ± 0.01	0.02	0.06 ± 1	0.03 ± 0.01
SO$_4^{2-}$	1.46 ± 0.89	4.35 ± 0.83	5.5 ± 1.5	0.31 ± 0.01	1.07 ± 0.03	1.9 ± 0.3

[a] LOQ: Limit of Quantification

Table S9. PS 1-PS 8 leachates cations concentration given in mg/L, determined via ion chromatography.

Cation	PS 1	PS 2	PS 3	PS 4	PS 5	PS 6	PS 7	PS 8
Na$^+$	58 ± 16	11 ± 5	100 ± 70	12 ± 2	21 ± 2	12 ± 1	72 ± 4	2.9 ± 0.9
NH$_4^+$	0.012 ± 0.002	0.02 ± 0.01	0.02 ± 0.01	0.03 ± 0.01	0.018 ± 0.003	0.021 ± 0.003	0.11 ± 0.01	0.03 ± 0.01
K$^+$	38 ± 7	18 ± 8	80 ± 40	16 ± 3	44 ± 5	20 ± 3	114 ± 2	10 ± 2
Ca^{2+}	4.0 ± 0.4	11 ± 3	6 ± 3	13 ± 2	3 ± 1	24 ± 3	60 ± 20	14.9 ± 0.3

Table S10. PS 1-PS 8 leachates anions concentration given in mg/L, determined via ion chromatography.

Anion	PS 1	PS 2	PS 3	PS 4	PS 5	PS 6	PS 7	PS 8
F$^-$	3.6 ± 0.7	0.5 ± 0.3	2 ± 1	0.8 ± 0.2	1.25 ± 0.08	0.9 ± 0.2	3.2 ± 0.4	0.62 ± 0.09
Cl$^-$	23 ± 9	14 ± 8	140 ± 100	16 ± 2	12.3 ± 0.3	40 ± 3	239 ± 10	6 ± 3
NO$_2^-$	0.031 ± 0.004	0.016 ± 0.003	0.05 ± 0.02	0.023 ± 0.002	0.05 ± 0.01	0.011	< LOQ	0.03 ± 0.01
Br$^-$	0.04 ± 0.01	0.01 ± 0.01	0.10 ± 0.07	0.0109 ± 0.0003	0.003 ± 0.001	0.013 ± 0.002	0.11 ± 0.01	0.008 ± 0.003
NO$_3^-$	2 ± 2	0.7 ± 0.3	5 ± 4	0.8 ± 0.1	6.27 ± 0.02	1.7 ± 0.2	5.4 ± 0.2	0.27 ± 0.07
PO$_4^{3-}$	0.3 ± 0.2	0.0293 ± 0.0004	0.11 ± 0.05	0.05 ± 0.01	0.385 ± 0.002	0.05 ± 0.01	0.01 ± 0.01	0.040 ± 0.003

SO_4^{2-}	19 ± 8	3 ± 1	30 ± 20	3.7 ± 0.2	2.24 ± 0.08	19 ± 5	101 ± 54	4 ± 1

Table S11. VN 2-VN 5 leachates cations concentration given in mg/L, determined via ion chromatography.

Cation	VN 2	VN 3	VN 4	VN 5
Na^+	6.5 ± 0.7	2.1 ± 0.1	16 ± 1	4 ± 1
NH_4^+	0.06 ± 0.02	0.024 ± 0.005	0.020 ± 0.005	0.02 ± 0.01
K^+	28 ± 1	7.6 ± 0.3	43 ± 2	12 ± 2
Ca^{2+}	19 ± 2	14.1 ± 0.7	5 ± 1	3.6 ± 0.1

Table S12. VN 2-VN 5 leachates anions concentration given in mg/L, determined via ion chromatography.

Anion	VN 2	VN 3	VN 4	VN 5
F^-	1.0 ± 0.4	0.54 ± 0.05	1.9 ± 0.2	1.23 ± 0.35
Cl^-	1.7 ± 0.4	1.61 ± 0.04	8.11 ± 0.39	1.373 ± 0.003
NO_2^-	0.038 ± 0.002	0.02 ± 0.01	0.0338 ± 0.0002	0.028 ± 0.003
Br^-	< LOQ[a]	< LOQ[a]	0.008 ± 0.002	0.009 ± 0.003
NO_3^-	50 ± 10	2.5 ± 0.8	6.9 ± 0.6	0.53 ± 0.02
PO_4^{3-}	0.4 ± 0.1	0.16 ± 0.04	0.18 ± 0.01	0.14 ± 0.06
SO_4^{2-}	4.04 ± 0.11	0.93 ± 0.09	1.48 ± 0.01	0.4 ± 0.2

[a] LOQ: Limit of Quantification

Correlation analysis

Table S13. Pearson correlation coefficients obtained from the ion concentrations coming from the leaching experiments. For the calculations, all the concentrations were expressed in millimolar units times the absolute charge of the ion (charge*mmol/L) and the appropriate ion balance was achieved assuming the HCO_3^- anions to be the amount corresponding to the cation excess.

Ions	F^-	Cl^-	NO_2^-	Br^-	NO_3^-	PO_4^{3-}	SO_4^{2-}	Na^+	NH_4^+	K^+	Ca^{2+}	Mg^{2+}
F^-	1	0.586	0.0377	0.395	-0.133	0.288	0.388	**0.818**	0.302	**0.771**	-0.00840	0.0164
Cl^-	0.586	1	-0.271	0.827	0.203	-0.149	**0.806**	**0.77**	0.612	**0.893**	0.511	0.469
NO_2^-	0.0377	-0.271	1	-0.111	-0.0886	0.49	-0.432	0.148	-0.439	-0.0144	-0.432	-0.366
Br^-	0.395	0.827	-0.111	1	0.589	-0.0903	0.861	0.61	0.327	0.641	0.728	0.72
NO_3^-	-0.133	0.203	-0.0886	0.589	1	0.244	0.682	-0.102	0.0834	0.0153	**0.884**	**0.918**
PO_4^{3-}	0.288	-0.149	0.49	-0.0903	0.244	1	-0.00929	0.103	-0.0731	0.105	-0.0148	0.0363
SO_4^{2-}	0.388	**0.806**	-0.432	0.861	0.682	-0.00929	1	0.428	0.525	0.615	**0.892**	0.881
Na^+	**0.818**	**0.77**	0.148	0.61	-0.102	0.103	0.428	1	0.232	**0.845**	0.0342	0.0239
NH_4^+	0.302	0.612	-0.439	0.327	0.0834	-0.0731	0.525	0.232	1	0.56	0.39	0.345
K^+	**0.771**	**0.893**	-0.0144	0.641	0.0153	0.105	0.615	0.845	0.56	1	0.239	0.235
Ca^{2+}	-0.008.40	0.511	-0.432	0.728	**0.884**	-0.0148	**0.892**	0.0342	0.39	0.239	1	**0.983**
Mg^{2+}	0.0164	0.469	-0.366	0.72	**0.918**	0.0363	**0.881**	0.0239	0.345	0.235	**0.983**	1

References

[1] "International Volcanic Health Hazard Network (IVHHN)", https://ivhhn.org/.
[2] F. Barberi, L. Leoni, *Bulletin of Volcanology* **1980**, *43*, 107–120.
[3] D. Miriello, D. Barca, A. Bloise, A. Ciarallo, G. M. Crisci, T. De Rose, C. Gattuso, F. Gazineo, M. F. La Russa, *Journal of Archaeological Science* **2010**, *37*, 2207–2223.
[4] G. Sen, *Petrology: Principles and Practice*, Springer Science & Business Media, **2013**.
[5] M. Kousehlar, T. B. Weisenberger, F. Tutti, H. Mirnejad, *Geofluids* **2012**, *12*, 295–311.
[6] S. E. Jorge-Villar, H. G. M. Edwards, *Philosophical Transactions of the Royal Society A: Mathematical, Physical and Engineering Sciences* **2010**, *368*, 3127–3135.
[7] R. L. Frost, M. L. Weier, P. A. Williams, P. Leverett, J. T. Kloprogge, *Journal of Raman Spectroscopy* **2007**, *38*, 574–583.
[8] R. L. Frost, J. T. Kloprogge, W. N. Martens, *Journal of Raman Spectroscopy* **2004**, *35*, 28–35.
[9] A. G. Gaydon, *The Identification of Molecular Spectra*, Springer Netherlands, **1976**.
[10] F. Menges "Spectragryph - optical spectroscopy software", Version 1.2.14, 2020, http://www.effemm2.de/spectragryph/R.

Author Contributions